# Investigation of mechanical and micro structural properties of ST14 steel sheet joints by friction stir welding process

**Mahmoud Afshari** ( m.afshari@aut.ac.ir )
Amirkabir University of Technology Department of Mechanical Engineering https://orcid.org/0000-0002-8556-4264

**Ehsan Salahshour Rad**
Malek Ashtar University of Technology Faculty of Materials Engineering

**Hossein Norozi Foroushani**
Amirkabir University of Technology Department of Mechanical Engineering

**Iraj Sattari Far**
Amirkabir University of Technology Department of Mechanical Engineering

**Original Article**

**Keywords:** FSW, ST14 steel, microstructure, tensile strength, hardness

**Posted Date:** October 7th, 2020

**DOI:** https://doi.org/10.21203/rs.3.rs-84022/v1

# Abstract

High strength and ductility are some of reasons that make ST14 steel one of the most widely used steels in automotive and aerospace industries. FSW is one of the new methods of solid-state welding that is proposed as a method with desirable mechanical properties.

In this study, mechanical and microstructural properties of 1.5mm thick ST14 steel sheets were investigated in the friction stir welding process. The results showed that the welded specimen with rotational speed of 800 rpm and linear motion speed of 80 mm/min had the highest tensile strength of 305MPa. In addition, results of metallographic test showed that the sample with 1000 rpm rotational speed and 50 mm/min linear motion speed had the highest heat input to the piece, and therefore the tungsten carbide particles were separated from the instrument and entered the stirred zone. Also the results of micro hardness test showed that in the welded specimen with rotational speed of 1000 rpm and linear motion speed of 50 mm/min, hardness increased to 115H1 HV in the stirred zone, which is higher than hardness of other samples in same region. It can be claimed that tungsten carbide particles are present in this area.


# 1. Introduction

Friction stir welding (FSW) is one of the relatively new methods of solid-metal bonding. Today, this method has found many applications in various industries such as shipbuilding, aerospace, automotive and rail, due to its many advantages such as no need for consumables, desirable mechanical properties and high distortion reduction (Nandan et al. 2008; Jadhav, and Dalu 2014; Roldo and Vulić 2019).

In this method, a wear-resistant and rotating tool with a specific geometry at the pin and shoulder penetrates the joint section of the connecting parts and moves along the connection path. The friction between the workpiece and the tool causes heat, which creates heat to soften the edge of the joint, and as the tool rotates, the material moves and creates the joint (Besharati-Givi and Asadi 2014; Pietras and Rams 2016). Figure 1 shows the general process of doing this process.

In recent years, much research has been done on the FSW process. Reynolds et al. (2003) investigated the feasibility of bonding DH36 carbon steel sheets to 304 stainless steel sheets by the FSW process. The results of their studies showed an improvement in the mechanical properties of the joints. Sahin et al. (2005) investigated the parameters affecting the bonding of high speed steel sheets to plain carbon steel by FSW. The results of his studies showed that the highest tensile strength is obtained at 600 MPa frictional pressure and 3.7 seconds at frictional time. Ueji et al. (2006) performed FSW on three plain low carbon steel annealed, cold worked and quenched at different rotational speeds. Their results showed that at the same rotational speeds, the quenched specimen had a wider modified area than the annealed and cold worked specimens. Meshram et al. (2013) investigated the bond toughness of Grade 250 steel sheets in the FSW process. Chansoria et al. (2015) investigated the parameters affecting the transient temperature distribution in friction welding of 304L stainless steel. Their results showed that increasing

tool rotation speed and decreasing travel speed and increasing normal force and shoulder radius increase the temperature peak.

In this study, due to the sensitive application of ST14 steel in the industry and lack of sufficient information for strength of the welded joints of these steels, a study was conducted to obtain suitable welding parameters and determine the mechanical properties of the welded piece.

# 2. Experimental Procedure

Increasing knowledge and numerous experiments have led to the use of various tools with different geometries and materials such as tungsten carbide in the FSW process of steels. Tungsten carbide is also used in this research. The geometrical parameters of the instrument used in this study are shown in Table 1.

Table 1
Geometric parameters of the tool used for the welding process.

| Diameter of the tool shoulder)mm( | Diameter of tool pin )mm( | Tool Pin Length (mm) | Angle of tool shoulder cone )degree( |
|---|---|---|---|
| 14.2 | 3.9 | 1.3 | 5 |

The dimensions of the ST14 steel sheets used as a workpiece in this study were 160 × 80 × 1.5 mm and were bonded to each other using a butt joint without any gaps. The chemical composition analysis of ST14 steel is given in Table 2.

Table 2
Chemical composition of ST14 steel (by weight percent).

| Element | Fe | C | Si | Mn |
|---|---|---|---|---|
| % wt. | base. | 0.04 | 0.01 | 0.23 |
| P | Ni | Mo | Cu | V |
| 0.007 | 0.03 | 0.01 | 0.03 | 0.002 |
| W | Co | Al | Sn | Pb |
| 0.003 | 0.004 | 0.055 | 0.007 | 0.003 |

A manual milling machine was used to make the rotational motion of the pins needed to connect the sheets. For fixing the sheets during the process, a fixture with dimensions of 600 × 400 × 2 mm was used. Talc powder was also used to prevent the sheets from adhering to the fixture during the welding process.

The values of the welding variables including tool rotational speed and linear motion velocity were chosen so as to have different modes of mechanical properties of the joints in the FSW process. The tool deflection angle was considered constant in all tests equal to 2 degrees. Table 3 shows the values of the parameters for different welding states.

Table 3
Variable values for different welding states.

| Sample no. | rotational speed (rpm) | linear motion speed (mm/min) |
|---|---|---|
| 1 | 1000 | 50 |
| 2 | 500 | 100 |
| 3 | 1000 | 100 |
| 4 | 800 | 80 |

Then the normal tensile test specimens were prepared transversely according to ASTME8 standard to evaluate the mechanical properties of the bonded sheets (Fig. 2).

Metallographic tests were performed to investigate the microstructure of base metal, weld metal, thermo-mechanically Affected Zone, and microstructural changes of the cross-sections of the samples. Subsequently, samples of appropriate dimensions were prepared and mounted. The surfaces were grinded using silicon carbide sandpaper (80 to 3000) and then polished with 0.3-micron alumina powder. The samples were etched with Nital solution containing 2% nitric acid and 98 ml of alcohol for 30 seconds to reveal the microstructure of base metal and weld metal. Then the microstructure of the different parts of the welded parts was examined and analyzed by Olympus optical microscopy (ck40m model) at different magnifications. The Buehler hardness tester was used to measure the micro hardness of the specimens and to draw the hardness profile of the weld sections and the Vickers micro hardness test was performed on the specimens. In this experiment, the specimens were prepared perpendicular to the central welding line and included base metals, weld metal, thermo-mechanically affected zone. In the hardness test, weights of 100 gr were applied to all specimens for 15 seconds at the time of force application and at a distance of 0.75 mm from the workpiece surface (center line in thickness). Also, the test intervals on each sample were 1 mm. The results of this experiment are presented as hardness profiles for all samples in the results section.

# 3. Results And Discussion

# 3.1. Investigation of the effects of welding parameters on tensile strength

Table 4 shows the results of the uniaxial tensile test on the joints as well as the failure site of the specimens.

Table 4
Results of uniaxial tensile test and location of joint failure.

| Sample no. | Ultimate tensile strength of the joints )MPa( | Location of failure |
|---|---|---|
| 1 | 270 | Base Metal |
| 2 | 91 | Weld metal |
| 3 | 299 | Base Metal |
| 4 | 305 | Base Metal |

According to Table 4, it can be said that the sample (4) has the highest tensile strength of 305 MPa with a rotational speed of 800 rpm and linear motion speed 80 mm/min. In order to compare the strength of the welded samples and the base metal, the base metal sample was also subjected to uniaxial tensile test and it was observed that the base metal had a tensile strength of 303 MPa, therefore, it can be said that the tensile strength of the sample (4) is approximately 101% of the base metal.

# 3.2. Microstructure analysis of ST14 welded steel joints

Figure 3 shows the optical microscopy image of the 14ST base metal cross section. As it is known, the microstructure has ferrite phase and due to very low carbon content (0.04%) the amount of pearlite phase is negligible. According to the lever rule in the Fe-C diagram, the structure appears to contain 2% pearlite phase and 98% ferrite phase.

Figure 4 shows the optical microscopy image of the cross-section sample (4). Due to the heat generated and the thermomechanical operations, different zones with different properties have been created at the junction. Therefore, it is expected that ferrite grains grow and become larger. On the other hand, by rotating the pin and shoulder in the Stirred Zone (SZ), thermomechanical operations are performed, which results in recrystallization in the grains and fine-grained up to 10–20 times, which enhances the mechanical properties of the joint. A little further away is the Thermo Mechanically Affected Zone (TMAZ). This area is affected by heat and mechanical operations at the same time, but its intensity is much lower than in SZ. The Heat Affected Zone (HAZ), located between the base metal and TMAZ, is only affected by heat and no mechanical operations are performed in this area. As can be seen in this area, in some parts, the grain size is more elongated and larger than the base metal or at least equal to the base metal.

For comparison the effect of welding parameters, optical microscopic image of a cross section of the sample no (1) was also examined (Fig. 5).

It seems that due to lower linear motion speed and higher rotational speed in this case, the heat input to sample (1) is also higher than other samples. For this reason, it is expected that as the input heat increases, the temperature of the tungsten carbide tool will also rise due to high friction, Causing the tool to soften and also some of the tungsten carbide material to be removed and entered to the Stirred Zone, and ultimately affect the bonding properties and reduce the strength. Also, because heat is high, it is

expected that grain growth in the SZ will be higher and the hardness will decrease in this area, but unexpectedly, the hardness of the area has increased significantly, which appears to be related to the tungsten carbide particles removed from the tool, that is visible in the form of black particles.

## 3.3. Survey hardness profile of ST14 welded joints

The hardness profile of the cross-section of the welded specimens is given in Figs. 6–9.

It should be noted that the average hardness of the ST14 steel sheet is equal to 91.5 and equal to the hardness profile of the specimens as the hardness of the weld metal increased in all four welded specimens compared to the base metal, which is the cause. It can be the microstructural changes that occur during the welding process, which greatly reduces the grain size in the weld area. As mentioned earlier, in sample (1), the hardness of the perturbation zone increased due to the separation of tungsten carbide particles from the tool and the composite formation of iron and tungsten carbide. In sample (2) also, due to the low rotational speed and the high speed of linear movement of the inlet heat to the sample, the lack of sufficient heat in the area in question caused the turbulence between the two samples to not proceed well.

Also because the structure in the SZ region is fine, the hardness has increased, but due to the lack of sufficient perturbation, the sample is not robust enough.

In Examples (3) and (4), the structure in the SZ region has been fine-grained due to thermomechanical operations, but the hardness in the area has increased, but the hardness in the TMAZ and HAZ has gradually decreased with the departure of the central welding line.

# 4. Conclusion

In this study, mechanical and microstructural properties of ST14 steel sheet joints were investigated by frictional welding process. For this purpose, the effects of linear motion velocity and rotational speed of the tool on the tensile strength and hardness of the weld joint of the welded joints were investigated and the following results were obtained:

1- The maximum tensile strength of the ST14 steel sheet joints was obtained by FSW at a linear movement speed of 80 mm / min and a rotational speed of 800 rpm at 305 MPa.

2- The hardness of the perturbed region is higher in the welded sheets than in the base metal. On both sides of the weld line, the heat-affected zone has a lower hardness than the base metal because of its coarser grain area.

3- The results of different tensile and hardness tests all indicate that the frictional disturbance parameters (tool rotational speed and linear motion velocity in this study) have a significant effect on the quality and properties of the joint.

# Declarations

Not applicable.

# References


1. Nandan, R., DebRoy, T. and Bhadeshia, H.K.D.H., (2008). Recent advances in friction-stir welding–process, weldment structure and properties. *Progress in materials science*, 53(6), pp. 980–1023, doi:10.1016/j.pmatsci.2008.05.001.
2. Roldo, L. and Vulić, N., (2019), Friction Stir Welding for Marine Applications: Mechanical Behavior and Microstructural Characteristics of Al-Mg-Si-Cu Plates. *Transactions on maritime science*, 8(01), pp. 75–83, doi: 10.7225/toms.v08.n01.008.
3. Jadhav, G.C. and Dalu, R.S., (2014), Friction Stir Welding–Process Parameters and its Variables: A Review. *International Journal of Engineering and Computer Science*, 3, pp. 6325–6328.
4. Pietras, A. and Rams, B., (2016), FSW Welding of Aluminum Casting Alloys. *Archives of Foundry Engineering*, 16(2), pp. 119–124, doi: 10.1515/afe-2016-0038.
5. Besharati-Givi, M.K. and Asadi, P., (2014), Advances in friction-stir welding and processing. 1st Edition, *Woodhead Publishing Series in Welding and Other Joining Technologies*, Elsevier,
6. Mishra, R.S. and Ma, Z.Y., (2005), Friction stir welding and processing. Materials Science and Engineering *Faculty Research & Creative Works*, 50(1–2), pp. 1–78, doi: 10.1016/j.mser.2005.07.001.
7. Reynolds, A.P., Tang, W., Posada, M. and DeLoach, J., (2003), Friction stir welding of DH36 steel. *Science and technology of welding and joining*, 8(6), pp. 455–460, doi: 10.1179/136217103225009125.
8. Sahin, M., (2005), Joining with friction welding of high-speed steel and medium-carbon steel. *Journal of Materials Processing Technology*, 168(2), pp. 202–210, doi: 10.1016/j.jmatprotec.2004.11.015.
9. Ueji, R., Fujii, H., Cui, L., Nishioka, A., Kunishige, K. and Nogi, K., (2006), Friction stir welding of ultrafine grained plain low-carbon steel formed by the martensite process. *Materials Science and Engineering: A*, 423(1–2), pp. 324–330, doi: 10.1016/j.msea.2006.02.038.
10. Meshram, S.D., Reddy, G.M. and Pandey, S., (2013), Friction stir welding of maraging steel (Grade-250). *Materials & Design*, 49, pp. 58–64, doi: 10.1016/j.matdes.2013.01.016.
11. Chansoria, P., Solanki, P. and Dasgupta, M.S., (2015), Parametric study of transient temperature distribution in FSW of 304L stainless steel. *The International Journal of Advanced Manufacturing Technology*, 80(5–8), pp. 1223–1239, doi: 10.1007/s00170-015-7102-6.


# Figures

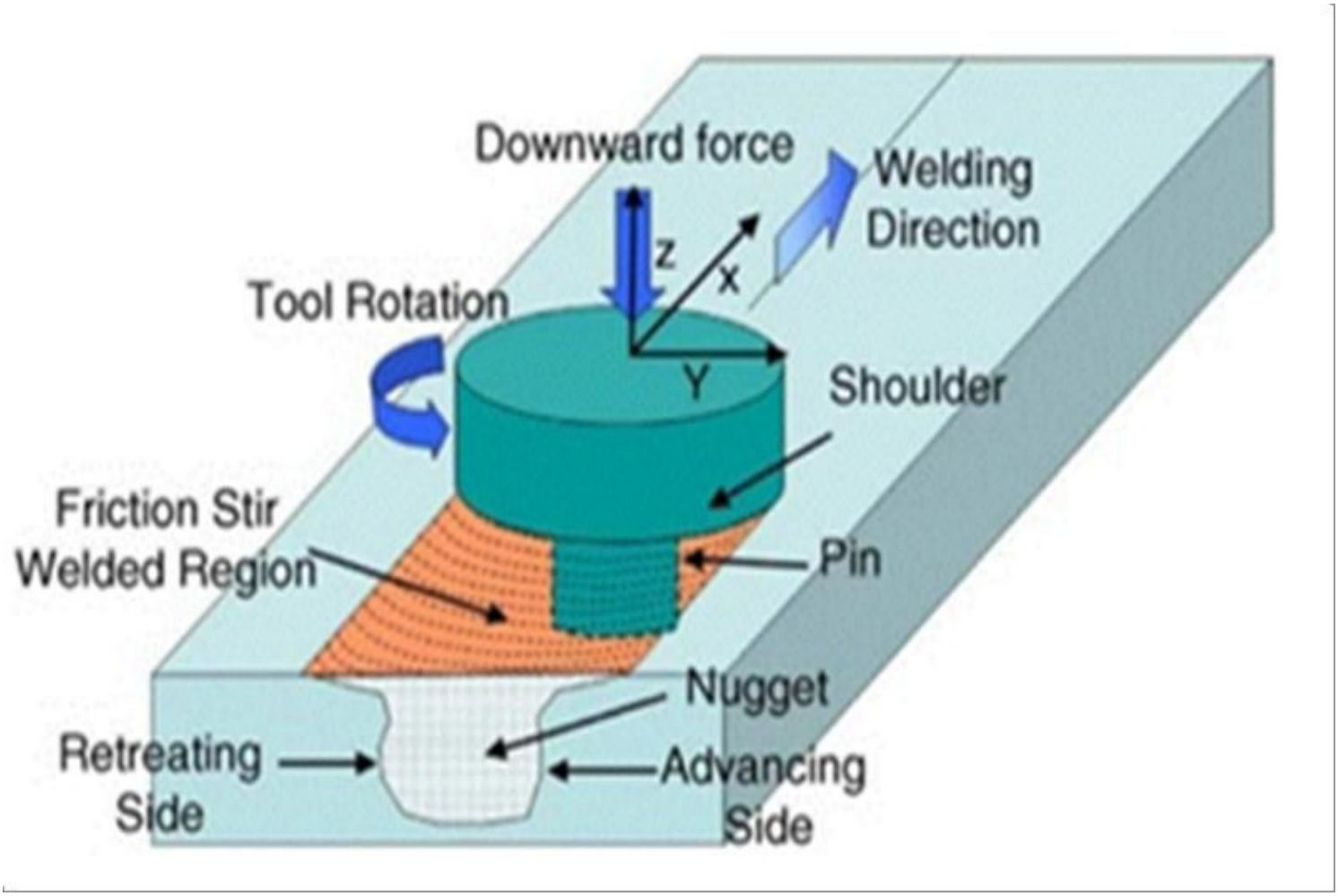


**Figure 1**

Schematic of the friction-welding process.


**Figure 2**

Welded tensile test specimens according to ASTME8.

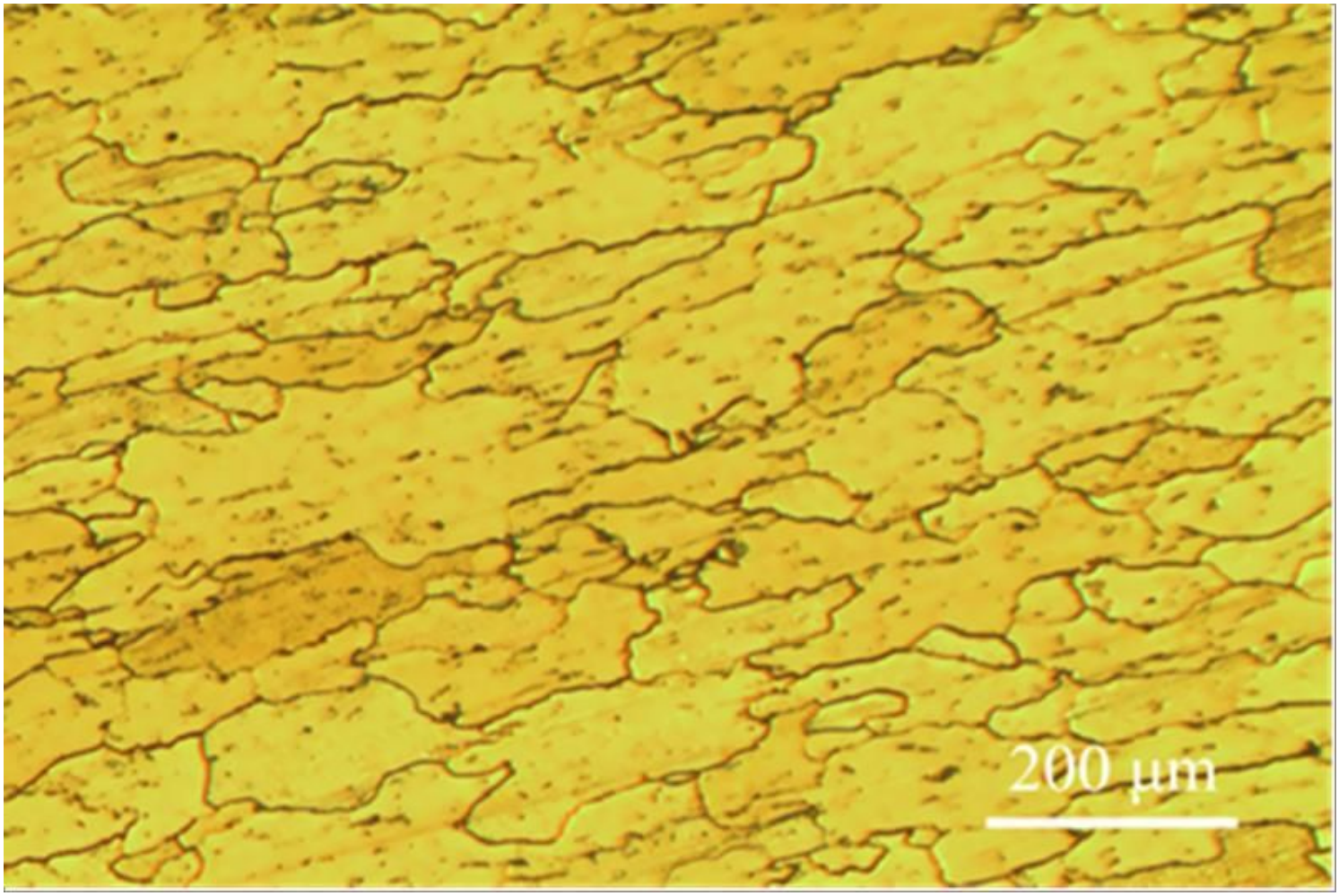


**Figure 3**

Microstructure of ST14 steel cross section (base metal).

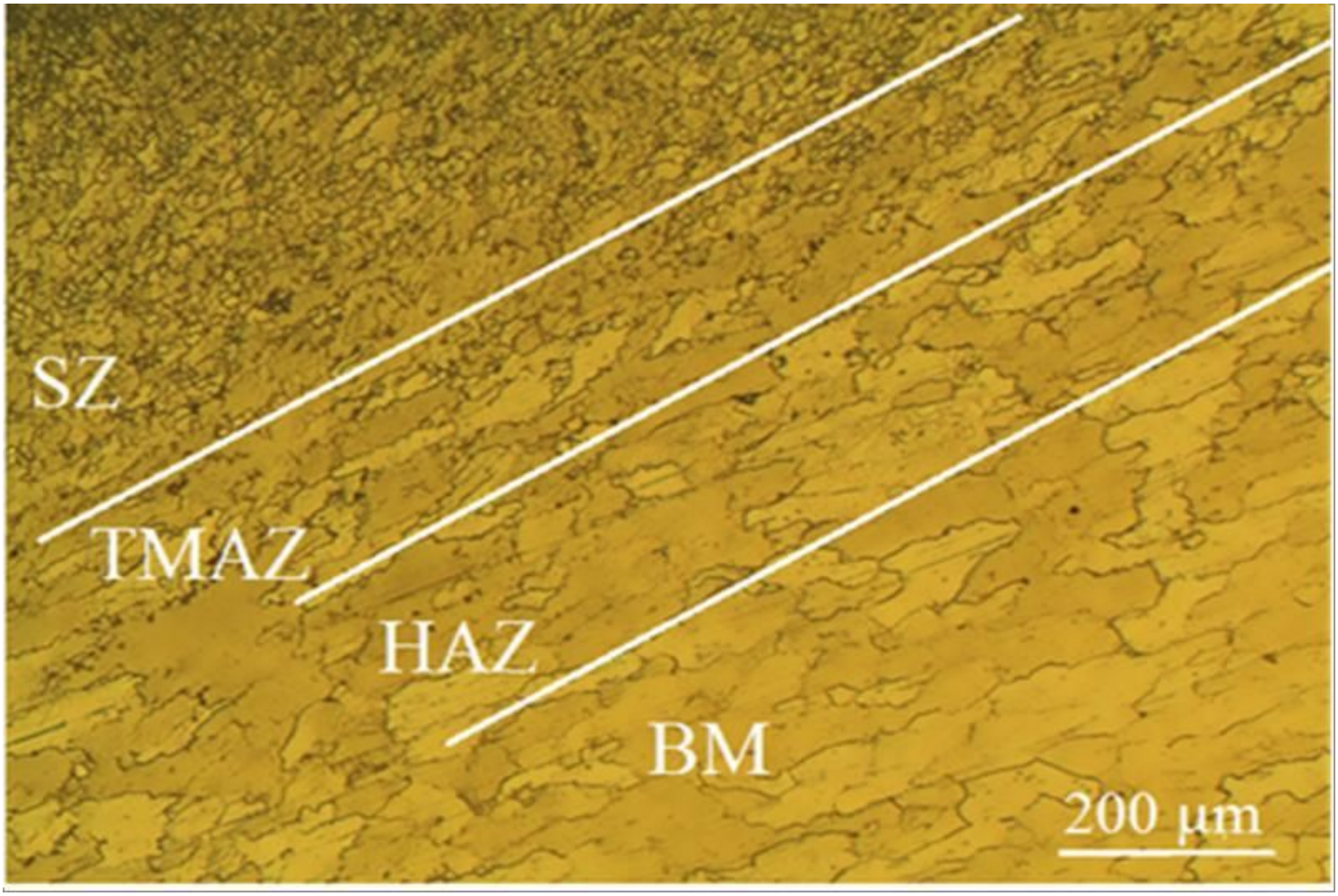


**Figure 4**

Microstructure of cross-section sample no (4).

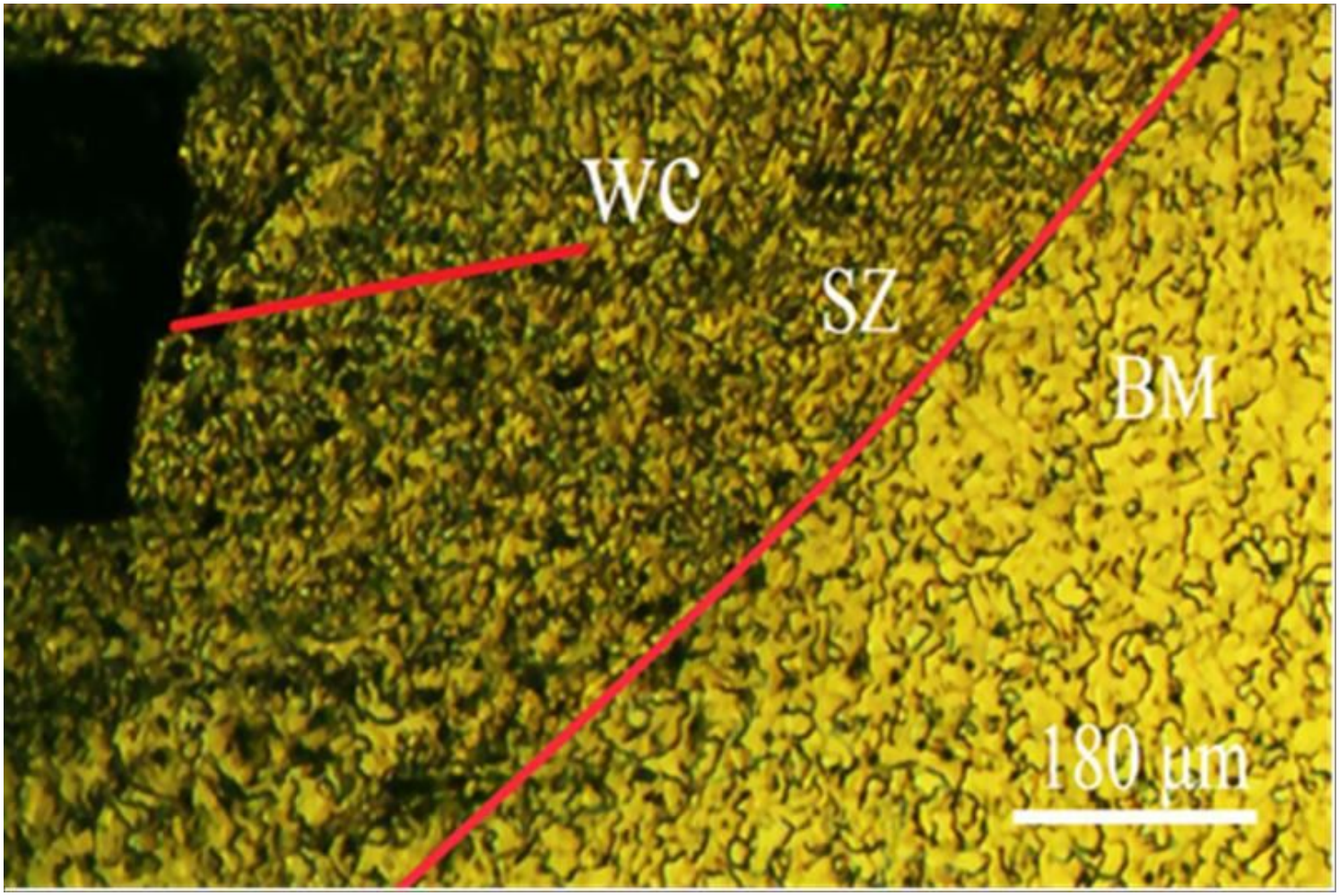


**Figure 5**

Microstructure of cross-section sample no (4).

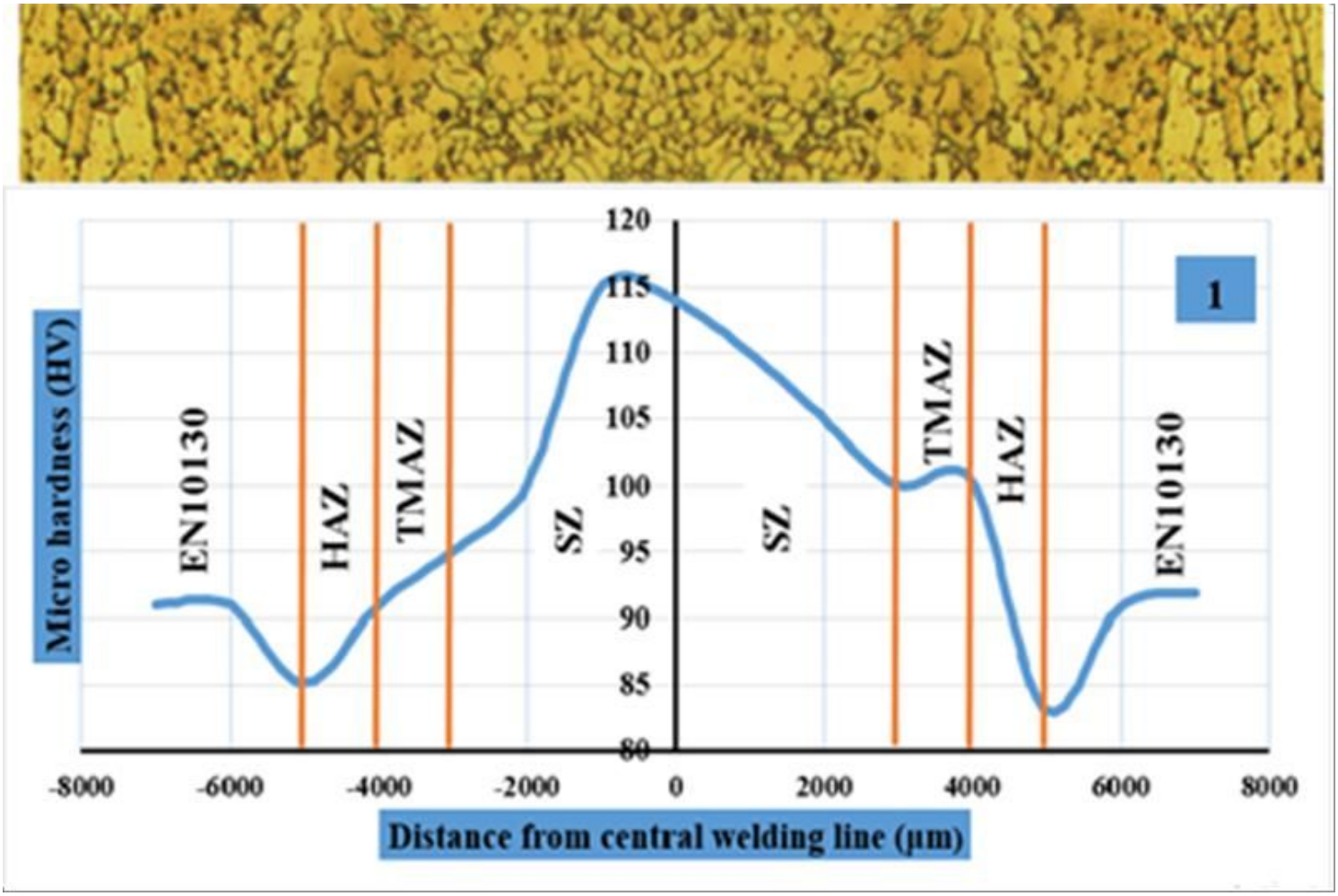


## Figure 6

Hardness profiles of connection cross section Sample 1.

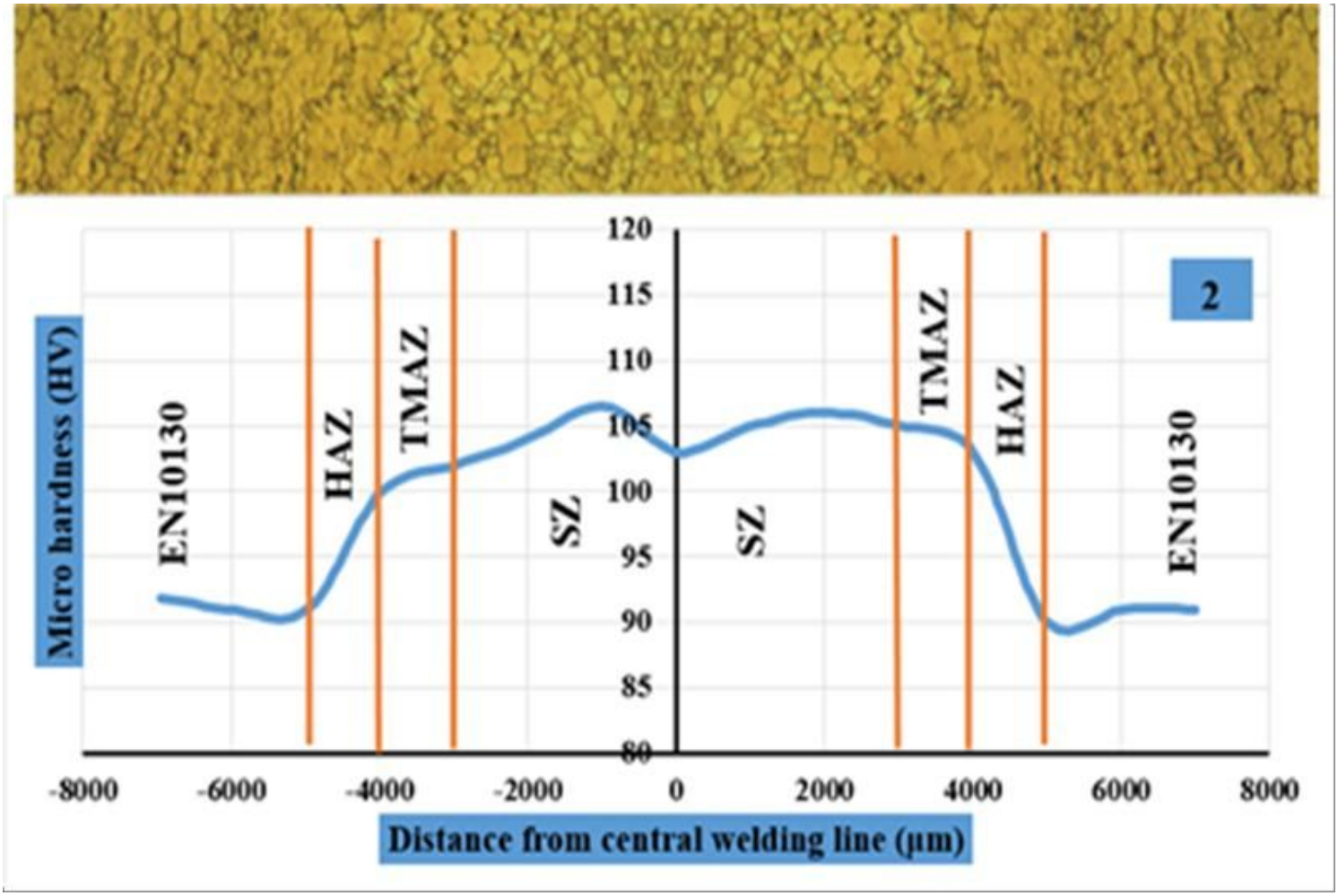


## Figure 7

Hardness profiles of connection cross section Sample 2.

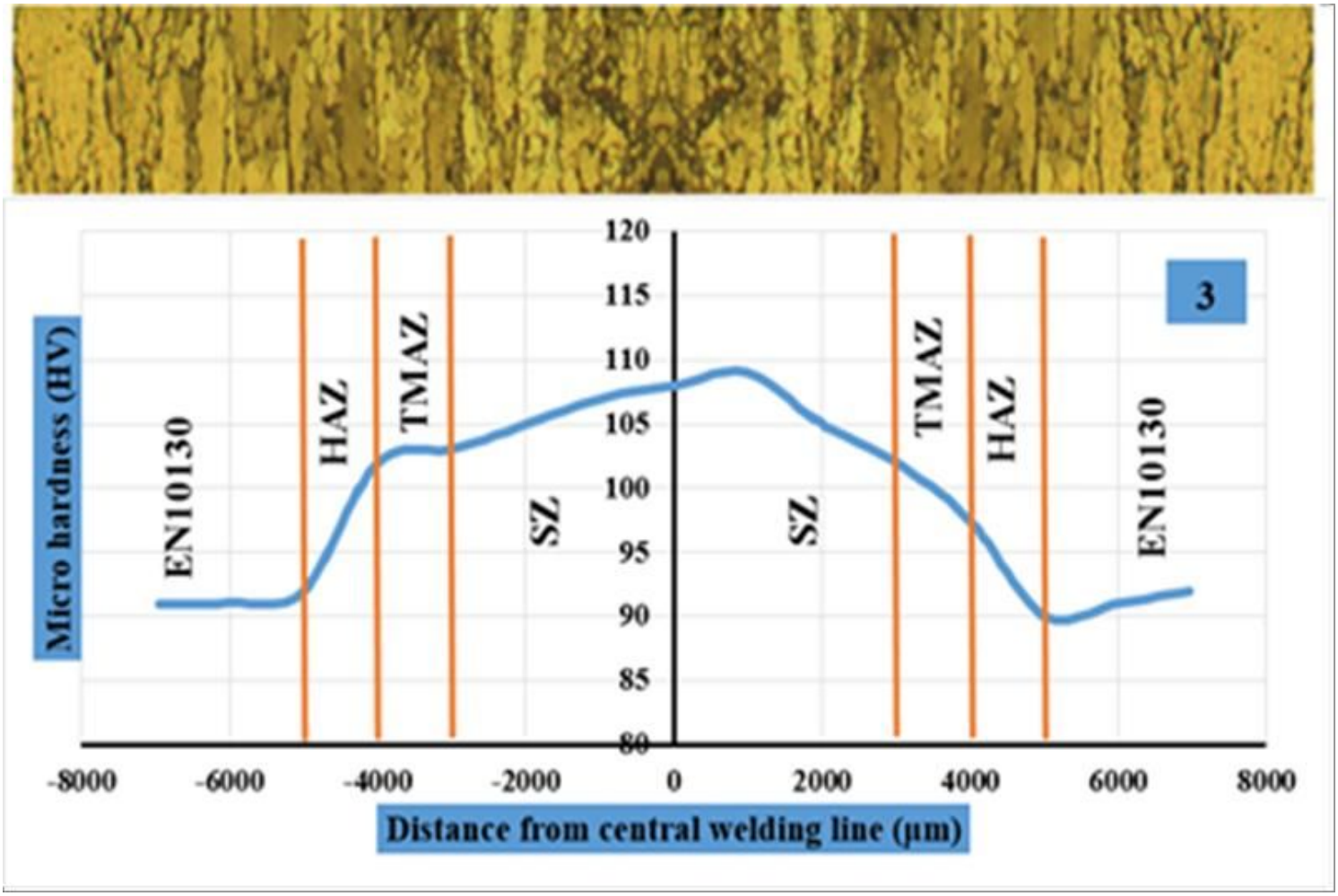


## Figure 8

Hardness profiles of connection cross section Sample 3.

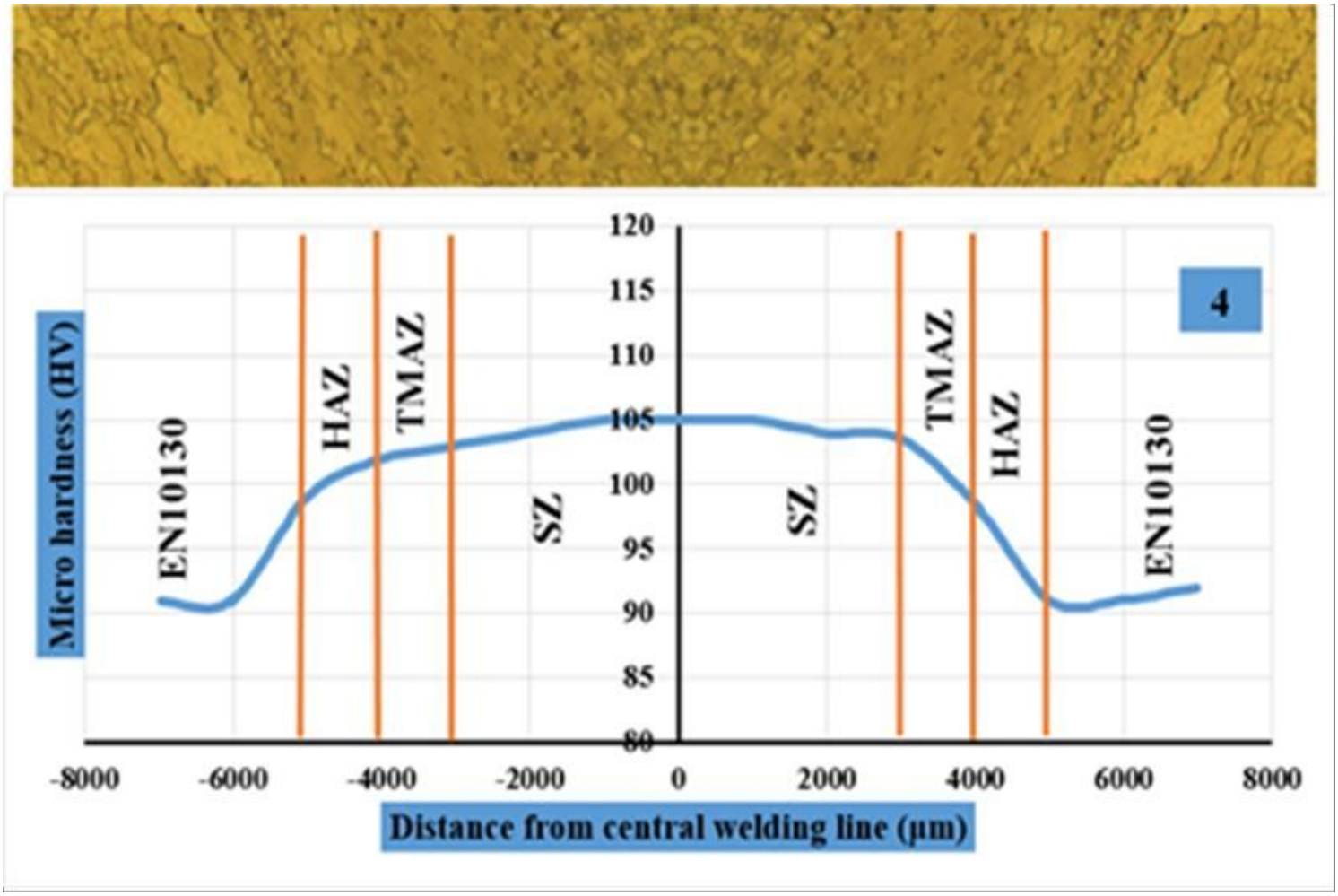


**Figure 9**

Hardness profiles of connection cross section Sample 4.